

Computational study of the Transmission pole during downburst using ANSYS, considering fluid-structure interactions

Akhilesh¹, S. Narayan^{2,*}

¹Department of Civil Engineering, M.Tech student, National Institute Technology Uttarakhand, Srinagar 246174, India

²Department of Civil Engineering, Assistant Professor, National Institute Technology Uttarakhand, Srinagar 246174, India

Paper ID - 140490

Abstract

A downburst is described as a strong downdraft that causes a devastating wind outburst on or near the earth surface. Such occurrences are more common during thunderstorms. Downbursts generally impinge on the ground and convect radially in all directions from the point of contact. Downbursts have been widely documented as a regular cause of high voltage electrical transmission tower and pole failures in numerous nations. The flow dynamics of impinging jets are investigated using numerical models, with applicability to downburst-related high intensity winds. The downburst is simulated using three primary viscous models ($k - \epsilon$, $k - \Omega$, and RANS). These three viscous models are used to simulate downburst in two dimensions. The RANS viscous model is used for further investigation. To determine the temporal variant characteristics of a downburst, both steady and transient state simulations are performed. The flow is quasi-periodic, with vortex rings formed by the initial jet instability impinging on the surface, where they find an unstable separation reattachment of the boundary layer. Fluid-structure interactions (FSI) are multiphysics problems that cannot be handled using single physics equations. To determine the impacts of downburst on transmission poles, a 2-D steel pole 8 metres high with a fixed base is put near the downburst. Downburst pressure is measured on a transmission pole. The stresses and deflections caused by the pressure distribution on the tower due to varying fluid domain dimensions and jet velocities on the transmission poles are determined using one way coupling, from 2-D transmission pole geometry to 3-D transmission pole geometry.

Keywords: CFD Analysis, Downburst, Fluid Structure Interaction, Impinging Jet, RANS viscous Model, ANSYS.

1. Introduction

Transmission line systems are essential for transmitting power from Power station to the end-users. Transmission line systems traverse tens of thousands of kilometers via a variety of terrains and climates. The transmission line system's structural components include the towers, conductors, ground wires, and insulator strings. Transmission line failures may have substantial social and economic consequences. Restoration of a tower necessitates a lengthy power outage, which in turn affect the power supply to end users and disrupting everyday life and causing significant economic loss. High-intensity wind (HIW), such as tornadoes and downbursts, is the cause of five out of six weather-related tower line failures. Wind load distributions for localised events deviate from the boundary layer wind profile used in structural design. Even though downbursts and tornadoes cause 80% of weather-related transmission line failures, most design wind standards do not estimate their loads [1]. Downburst winds have caused several transmission line failures around the world. Tornadoes and cyclones do not place a load on transmission towers as localised downbursts do. A downburst is a mass of cold and damp air that abruptly descends from the cloud base of a thunderstorm, impacts the ground, and then moves horizontally. A downburst is formed

by a column of sinking air that, upon striking the ground, disperses in all directions and can create destructive straight-line winds of over 240 km/h (66.66 m/s). Thus causing damage comparable to, but distinct from that caused by tornadoes, downburst. In the past, various studies have focused on the characteristics of the downburst. The cold air outflow from thunderstorms, later known as downbursts, was first described by Goff & Goff [2]. Gomes & Vickery [3] described a probabilistic approach to calculating the probability of an extreme wind speed under mixed wind circumstances.

Kim & Hangan [4] investigated the macro-flow dynamics and the scale dependency of impinging jets numerically to simulate downbursts. To identify critical features for assessing the effects of wind loading on structures, Zhang et al. [5] examined 277 wind speed data with strong transients and thunderstorm outflow labels. A method to extract the statistical characteristics of synoptic wind (cyclones and downbursts) from datasets of transient wind speed was proposed by Solari et al. [6]. Downbursts, one of nature's most dramatic and disastrous phenomena, and the wind stress they impose on structures were explored by Solari [7]. A two-fluid density-driven model was created by Babaei et al. [8] to

*Corresponding author. Tel: +919945670734; E-mail address: shashi.nituk@gmail.com

replicate the downburst as it is seen in nature. The largest datasets have been analysed by Canepa et al. [9], they concluded that impinging jets are reproduced as transient phenomena with a quick ramp-up of velocity, a velocity peak, a short statistically stagnant zone, and a final velocity deceleration, as predicted in downbursts. They also observed that the big vortex is frequently preceded by a smaller surface vortex, depending on the downburst's radial distance.

The collapse of various transmission towers during downbursts has drawn researchers' attention to the behavior of different structures during tornados. Shehata et al. [10] used numerical models to assess transmission tower performance under downburst loads. They translated wind velocity data into static forces acting on the tower. Shehata & El Damatty [11] investigated the effect of various downburst parameters on the performance of a guyed tower transmission line that fell after a downburst in 1996. Hamada & El Damatty [12] used a three-dimensional finite-element model to conduct a detailed examination of transmission line constructions under tornado stress. Aboshosha and El Damatty [1] investigated previous failure studies of Transmission Towers during downbursts and determined that differential stress in the related conductors is a common failure mechanism. Elawady & El Damatty [13] used nonlinear analysis to propose a simple method for estimating forces in conductors. Ibrahim [14] developed a non-linear finite element model to predict stress in pre-stressed concrete poles during a downburst. Ahmed et al. [15] evaluated wind turbines behaviour numerically during downbursts when a CFD model for downburst wind is combined with a wind turbine structural model.

The research presented above makes it abundantly clear that the downburst event is the root cause of the structure failures. Both the design and the analysis need to take this into account. In addition, there is a scarcity of literature concerning the stresses developed in the structures due to the downbursts. This study simulates the downburst by employing an impinging jet, as has been reported in literature using ANSYS Fluent [16]. In other words, the downburst is thought to be a strong gust of chilly wind moving at a particular speed. In order to replicate the downburst, several different viscous models are used. The effect of downburst on the transmission pole is investigated for various viscous models. Evaluation is done on the steady state and transient solution for the computational fluid dynamics. The model is validated by comparing it with the results that have been provided for the transient solution. A one-way interaction between the fluid and the structure is considered to evaluate the stresses and deformation of the pole for two distinct velocities.

2. Methodology

The current research is split into 3 sections in order to explore the Fluid Structure Interaction (FSI) between the transmission pole and downburst. 1) Verification of downburst simulation with the reported results. 2) The impact of various viscous models on the transmission pole during a downburst. 3) The interaction of the pole's structure with a downburst.

The Impinging Jet has been used to model the Downburst. To mimic the downburst at a certain speed, the diameter and velocity of the jet are assumed. The steady state and transient

analysis for the downburst is carried out. The reported results and the results of the CFD Analysis are compared. RANS model for the fluid is assumed in this study. Results like transient analysis at the lower time step are also given after the results have been validated. For the sake of completeness, the steady state solution for the Downburst simulation is also included in the next section.

In the second part a pole is inserted in the domain of study. In the current study, a transmission pole rather than a tower is assumed to speed up computation and concentrate on behavior. One could examine a transmission tower in the future. This is currently outside the scope of this paper. Most of transmission tower/poles failure is caused by downburst as uneven distribution of velocity on both side of pole generates net pressure force in one direction, leads to its failure. So, it is important to study the pole behavior under these high intensity winds (HIW) for future investigation. Downburst in this case is simulated by three different viscous models RANS, $K - \epsilon$ and $K - \Omega$ model, to see different effects. The CFD results for RANS model are compared with that of the $K - \epsilon$ model $K - \Omega$ model for the impact of downburst on transmission pole during a Downburst.

Fluid Structure Interaction (FSI) between the downburst and the pole is conducted in the last section. The interaction of fluids and solids is a phenomenon that is frequently seen in the natural world. For instance, the wind-related movement of sand dunes or the deformation of trees. A solid structure may deform as a result of fluid flow around or inside it in a system known as the interaction between fluid and solid. As a result, this deformation modifies the fluid system's geometry and boundary conditions. The solids are subjected to external pressure and undergo significant deformation as a result of the fluid flow dynamics, which also alters the boundary conditions and solid geometry. These concerns are referred to as fluid-structure interactions (FSI) problems. Both steady and oscillatory fluid-structure interactions are possible. In oscillatory interactions, the strain induced in the solid structure causes it to move when the stress is reduced, and the structure returns to its former state only for the process to repeat.

In general, problems involving fluid-structure interaction are Multiphysics issues that are particularly challenging to resolve analytically. In order to analyze them, either numerical simulations or experiments must be used. Fluid dynamics and structural dynamics are two disciplines that are involved in these Multiphysics challenges. Solids and fluids can be coupled in a one-way or two-way manner. Only the fluid pressure acting at the structure is transferred to the structure solver for one-way coupling calculations. The displacement of the structure is also sent to the fluid solver in two-way coupling calculations.

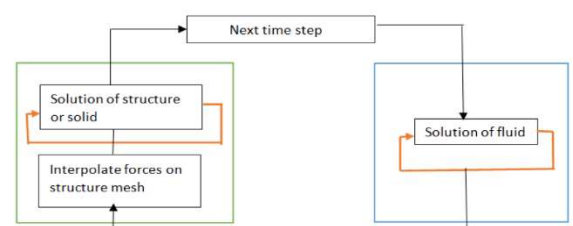


Figure 1. Steps of One-way coupling.

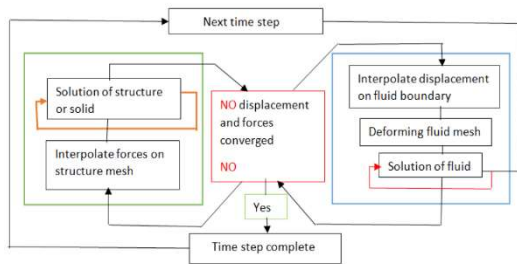


Figure 2. Steps of two-way coupling.

If the motion of a fluid flow is impacted by structural deformation and vice versa, the connection is said to be one-way. In Figure 1, the stages for one-way coupling are depicted. Fluid flow is first computed in this coupling approach up to the required convergence. After that, until convergence is achieved, the structural boundary conditions at the contact and their impacts are recalculated with the fluid flow calculations. Figure 2 shows the two-way coupling process in phases. In a two-way coupling, fluid flow and structural deformation both impact the solution at the same time. When the first step is executed, convergent solutions of the fluid flow have an impact on the solid body deformation. The structural solver's output is then derived from the fluid flow solution taking it into account as a boundary condition, and the fluid flow result is interpolated to the structural mesh at the interface as one-way coupling. As a result, the structure's mesh is displaced, and the fluid flow mesh is interpolated using the displacement values. Up till the requisite accuracy is attained, the process is iterated.

One-way coupling has been used in this study's work because it is easier and faster. However, both one-way and two-way coupling might be used for additional investigation. An accurate and economical simulation may be obtained with the help of a solid understanding of coupling methods. So, it is up to us to decide which approach suits the most, and one can choose the coupling method based on the requirements.

3. Numerical Results and Discussions

RANS viscous modal with specified parameters and boundary conditions is employed to simulate the downburst in Ansys [16]. A commercially available Computational Fluid Dynamics (CFD) software, Fluent, is employed to simulate the generic downburst/impinging jet flow. While three-dimensional (3D) vortex dynamics can be directly simulated for all scales using Direct Numerical Simulations (DNS) or over a range of scales using Large Eddy Simulations (LES), these simulations involve very high computational costs mostly for the large Reynolds numbers of cases investigated herein. Therefore, 2D model is created in ANSYS. The objective of the current study is to investigate the macro scale flow dynamics of an impinging jet as a generic case for downburst wind flow phenomena. Therefore, the time-filtered RANS equations were solved. Geometry is created of specified domain in Fluent and it is set in operations in Ansys for this 2D surface. In setup boundary

conditions are provided as shown in figure 3 with inlet velocity 6.1m/s computed for Reynolds no. of 20,000 as:

$$Re = \frac{V_{jet} D_{jet}}{\nu} \tag{1}$$

Here V_{jet} is jet velocity of downburst and D_{jet} is diameter of jet, ν is kinematic viscosity of air considered at 20deg. Reynolds stress model (RSM) was employed herein. Wall reflection terms were included. The default model constants used in the RSM were as follows: $C_{mu}=0.09$; $C1\text{-epsilon}=1.44$; $C2\text{-epsilon}=1.92$; $C1\text{-ps}=1.8$; $C2\text{-ps}=0.6$; $C1'\text{-ps}=0.5$, $C2'\text{-ps}=0.3$, turbulent kinetic energy (TKE) Prandtl number=1; turbulent dissipation rate (TDR) Prandtl number=1.3. These parameters are derived from Launder [17]. The detail of the model is discussed in the subsequent section.

3.1 Verification of CFD model

For downburst, transient state solutions are solved in order to examine downburst behavior. The transient solution is significant because it demonstrates how the ring vortex formed by the Kelvin-Helmholtz instability close to the wall impacts the wall and extends radially. Such fundamental ring vortices disrupt the boundary limit layer's equilibrium, creating an auxiliary vortex that separates and reattaches and extends outward until the vortex rings scatter. For various time intervals, transient solutions were recorded, demonstrating how downburst behavior evolved over time. Boundary conditions are defined as Velocity Inlet, Pressure outlet, slip wall, Wall as shown in figure 3. The inlet velocity of 6.1m/s is provided for Reynolds number of 20,000. At pressure outlet, gauge pressure is kept zero to make it atmospheric pressure. At wall, no-slip-wall boundary condition is provided to catch the behavior of viscous sublayer. And at slip wall, zero Specified shear in all directions is provided as for free flow of fluid. The geometry in figure 3 is symmetrical about central y-axis, so boundary conditions are same on both sides. The meshing and Reynolds number for transient solution is kept same as that of a steady state solution. Dimensions of the domain are also kept same as in steady state. Time step size is taken as 0.01 to capture slow behavior with number of time steps of 1300, to capture behavior up to 13 seconds and to provide time for generation of 2nd ring vortex. Maximum iteration per time steps is taken as 30 for convergence of solution at each time step. The other conditions are Turbulence intensity =1%; Hydraulic diameter =D, Pressure outlet Backflow turbulence intensity =1%. A domain of $10D \times 20D$ is solved using the Ansys fluent. The detail of the problem is shown in figure 3.

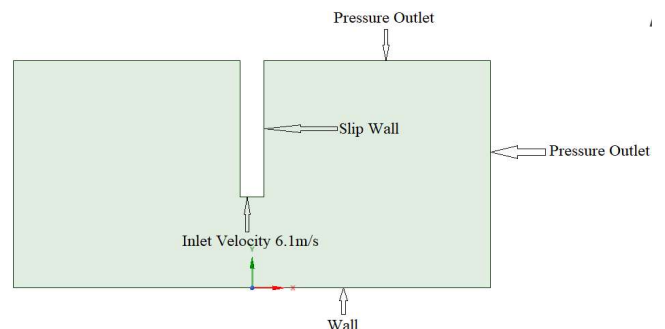
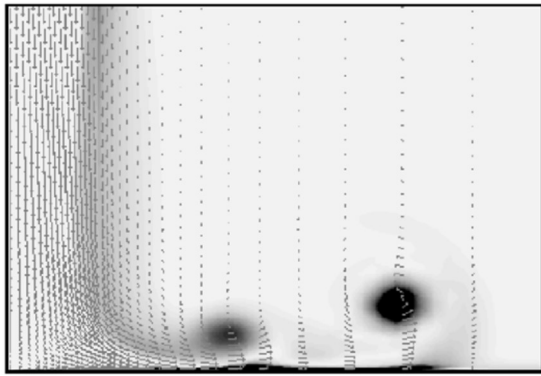
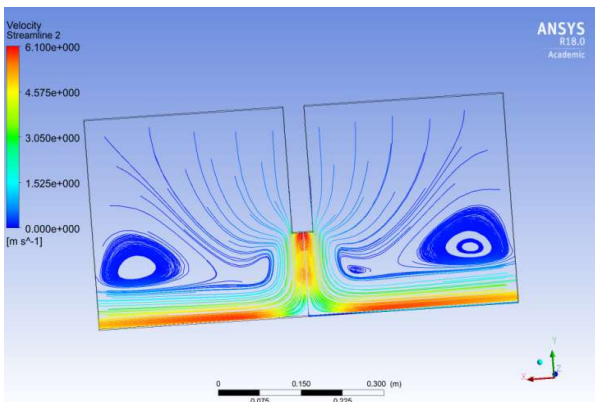


Figure 3 The Problem statement for validation.

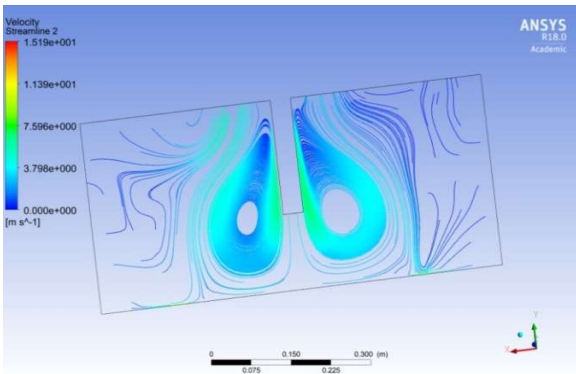


a)

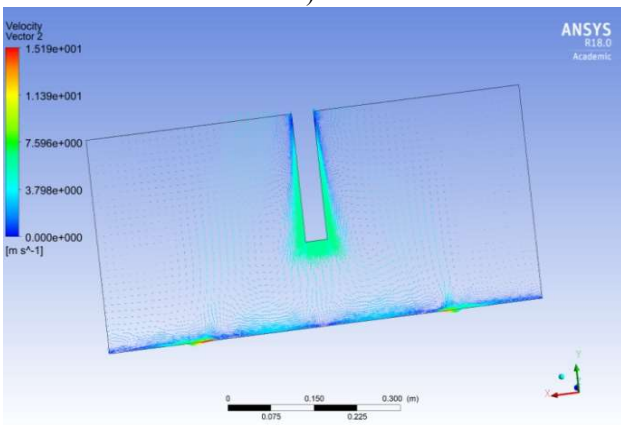


b)

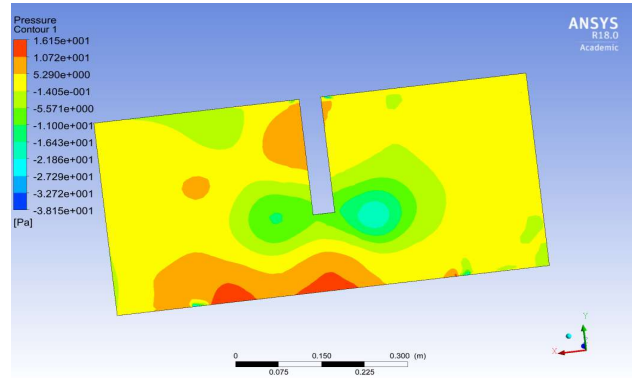
Figure 4 The Transient solution at 12.8sec a) as reported by Kim & Hangan [4] b) ANSYS CFD



a)



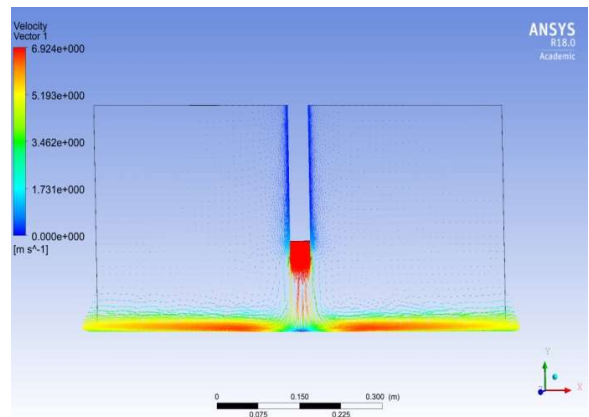
b)



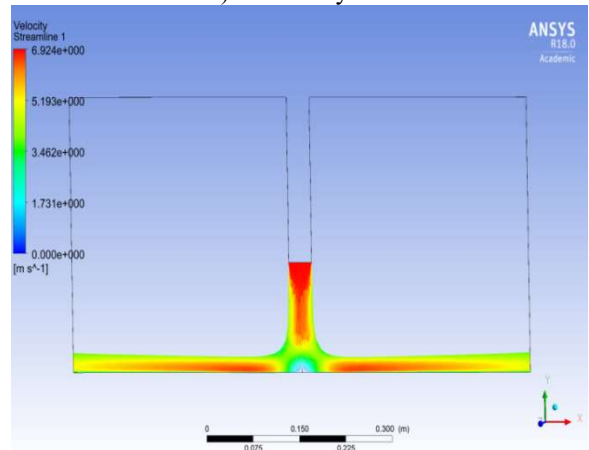
c)

Figure 5. a) Velocity Streamlines, b) Velocity Vectors and c) Pressure contours for steady state downburst

The model selected here for validation has been numerically investigated by Kim & Hangan [4]. In the present investigation, the full CFD model has been analyzed instead of a half model as evaluated by the Kim & Hangan [4]. This is purposefully done as the main objective of the paper is to observe the dynamic effects on the transmission pole at one side of the domain. In figure 4, the results of the CFD at 12.8s has been compared with that of the results reported. It can be observed from the figure 4 that at $t=12.8\text{sec}$, the generation of two vortex rings can be seen in both results due to Kelvin Helmholtz Instability i.e. generic case of impinging jet as defined in paper. The same has also been reported by Canepa et al. [9]. Moreover, The location of the vortex is also similar.



a) Velocity Vector 1



b) Velocity streamline 1

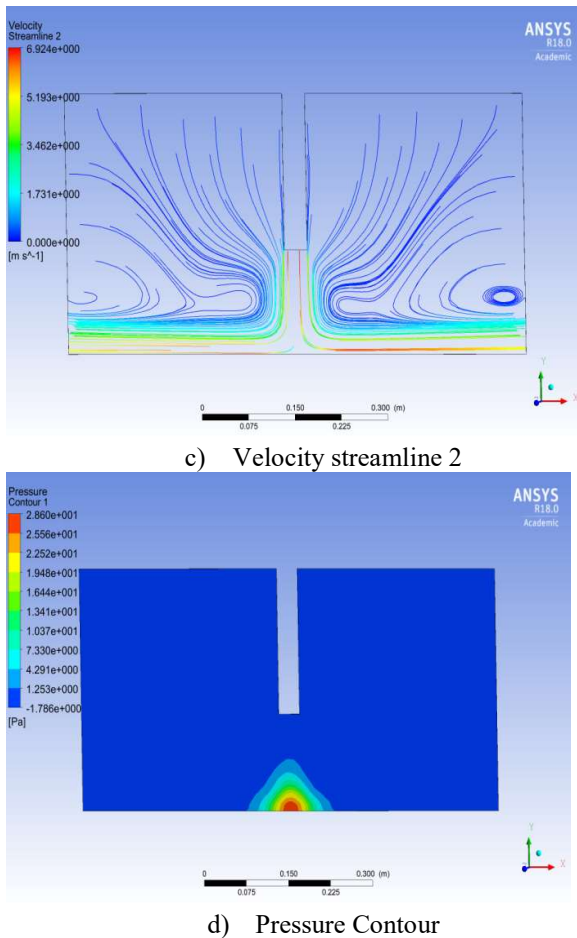


Figure 6. Showing Transient simulation results of downburst at $t=3.4$ sec

For completeness, the results for the steady and transient states at 3.4 seconds are also provided. Figure 5 depicts the downburst-generated velocity streamlines, velocity vector, and pressure contours on a 2D surface for the steady state solution. The maximum positive pressure regions are seen close to the wall, and the negative pressure regions are seen close to the downburst, indicating the effects of the downburst in the immediate area. The vortex is created by the areas of low pressure that are close to a downburst. It is also worth noting that one vortex forms in both halves of the domain near the inlet of the downbursts.

Figure 6 depicts the transient solution for the downburst at 3.4 seconds. The initial vortex can be seen to form close to the wall. Later, it moves in the direction of the center. Figure 6 depicts the beginning of the Kelvin-Helmholtz instability's role in the generation of the ring vortex near the wall. For an inlet velocity of 6.1 m/s for $Re=20,000$, maximum pressure, minimum pressure, and maximum velocity values are also displayed in the figures. Figures 4-6 show that the negative pressure is first noticed at the outer edges and gradually moves toward the center. Finally, it is seen close to the region where the downburst began. We observe maximum velocity of 15.1 m/s and a maximum positive pressure value of 16.5 Pa. Negative pressure zones are also created by downburst in the vicinity with maximum negative pressure value of 38.1 Pa.

3.2 Effect of Downbursts on the transmission pole

In this investigation, a transmission pole is positioned close to a downburst to observe the impact on the pole. The pole appears as a rectangle in 2D and has been used for simulation simulations. Three different viscous models, RANS, $k - \epsilon$ (Standard), and $k - \Omega$ (SST), are used to mimic downburst. The RANS model has been validated for the fluid dynamics in the previous section. Therefore, it is anticipated that the base for comparisons will be the RANS model's output. Geometry, Meshing and boundary conditions all are same in all three viscous models. Enhanced wall treatment is provided in wall treatment in all three models. Reynolds Stress model is provided in RANS, in K-epsilon Realizable is used and in k-omega SST model is used. The steady state solution for different models is presented here.

Figure 7 illustrates, for several models, how streamlines alter in relation to the pole near a downburst. RANS model gives better downburst simulation results than other models as shown in figure 7 and 8. Streamlines in RANS model gets deflected by pole as observed in normal wind condition and creating ring vortex in the surroundings. The ring vortex is also observed in the $k - \Omega$ (SST) model. According to results, the RANS model produces a more realistic pressure distribution induced by a downburst in the immediate vicinity than the other models. $k - \epsilon$ does not provide values correctly near wall as it uses viscous damping functions which do not work for every flow. However, it gives better results away from wall. *whereas*, $k - \Omega$ (SST) does not require damping functions close to the wall. It works well for separation close to the wall but not well enough elsewhere. The Reynolds Stress model, which is used in this situation, operates on the concept of mixing length provide good results in this case.

The pressure contours that a downburst produces in its immediate surroundings for the three different models under consideration are presented in Figure 8. Results shows max pressure value near tower for all the cases. This pressure will affect the tower and may cause their failure due to generation of high stress and strain. The stresses and strains caused by the downbursts are calculated further using one-way coupling FSI on the Transmission pole.

3.3 DOWNBURST EFFECTS ON TRANSMISSION POLE considering the FSI Effects.

As observed in the previous section, the RANS viscous model is best used for the current study while simulating downbursts using various viscous models. RANS Viscous model has therefore been used in subsequent research. Utilizing a one-way coupling technique, the strains and deflection of the transmission pole caused by the pressure created by the downburst are assessed. It is noted that the strains and deflection change as the velocities rise. Two different velocities have been considered for this. For all circumstances, boundary conditions and meshing are the same as before. There are no changes to any other inlet, outlet, or other conditions. The pressure that is generated on a transmission pole has a 2-D geometry, and the pressure that is transferred to the pole has a 3-D geometry with an 8-meter-high, 5-inch cross section. As the pole's base is supported by

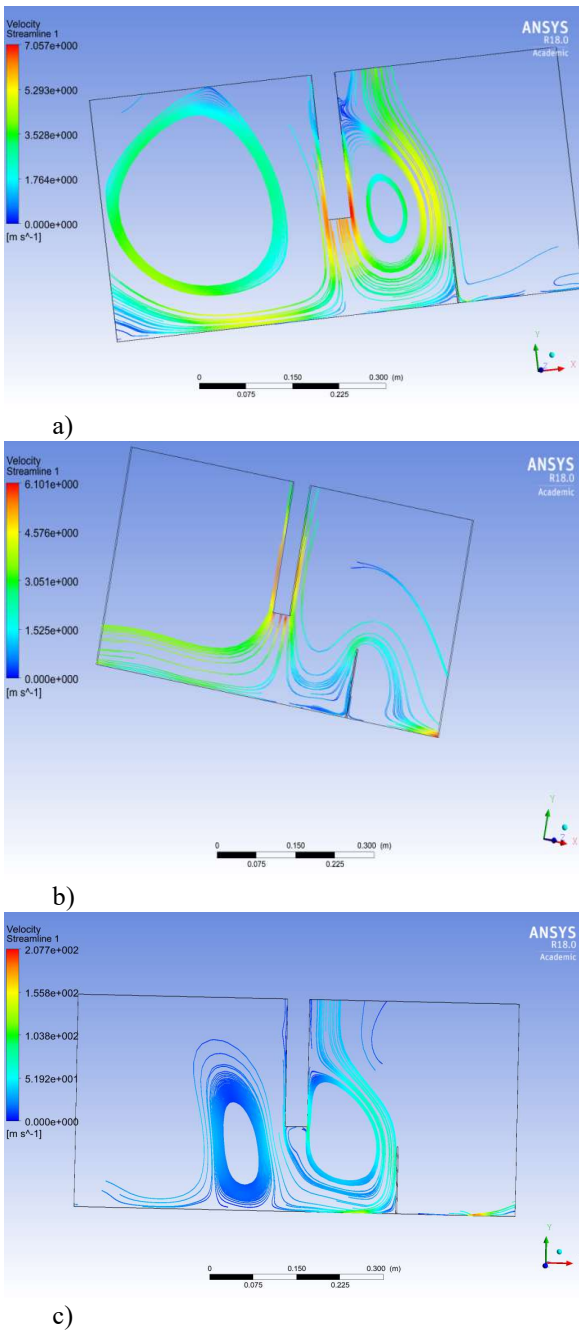


Figure 7. Streamlines comparison for different viscous modal: (a) RANS, (b) $K - \epsilon$ (Standard) and (c) $k - \Omega$ (SST)

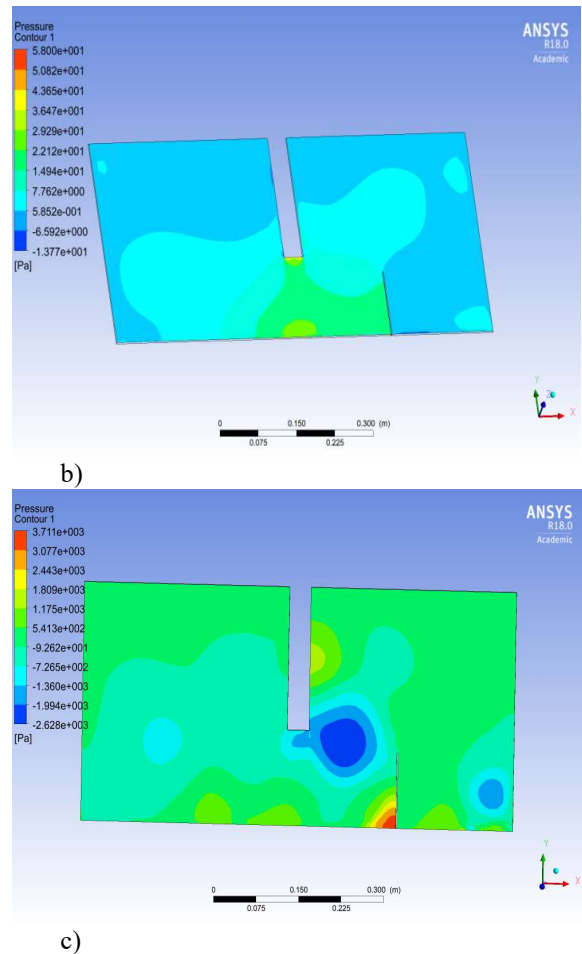
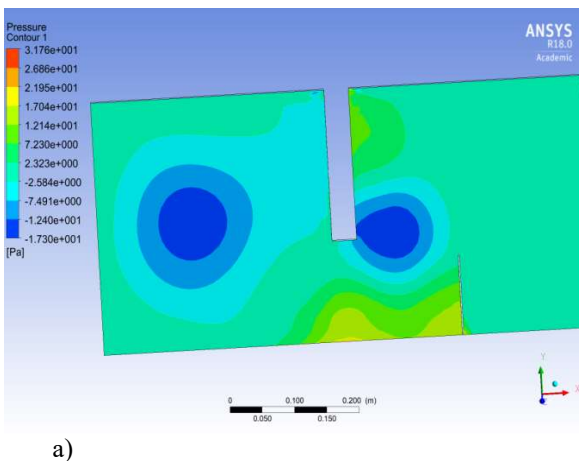


Figure 8. Pressure comparison for different viscous modal: (a) RANS, (b) $K - \epsilon$ (Standard) and (c) $k - \Omega$ (SST)

a rigid support, pressure is created on the pole's faces other than the base. To interpolate pressure values at the mesh nodes in static structure, fine mesh is formed in the pole. Calculations are made for Equivalent (Von-Mises) stress, Principal stress, and Total deflection values.

Case 1. - Downburst jet vel.-10m/s

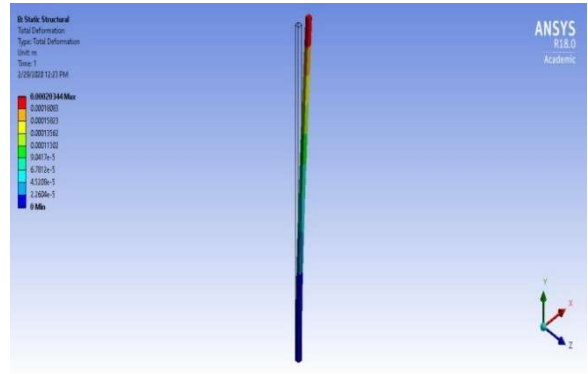
In this case for pressure generation on transmission pole by inlet jet velocity of 10m/s is taken for same flow domain. The pressure generated is coupled in static structural as a Multiphysics problem to find different stresses and deflection values. All other turbulent values and conditions are kept constant with same boundary conditions and stresses and deflection values are generated on the transmission pole. The results of CFD Solution are shown in figure 9. It can be seen from the figure 9 that there are several vortices formed during the steady state solution. It can be noted that the density of vortex formation in the vicinity of the pole is high. The von-Mises stress and maximum principal stress distribution over the solid elements on the pole is also shown in figure 9. It can be observed that the stress is in the range of 0.1-1MPa. The displacement profile at steady state is also shown in the figure 9 and the maximum displacement is 0.2mm for 10m/s impinging jet velocity.

Case 2. -Downburst jet vel.-100m/s

In this case for pressure generation on transmission pole by inlet jet velocity of 100m/s is taken.

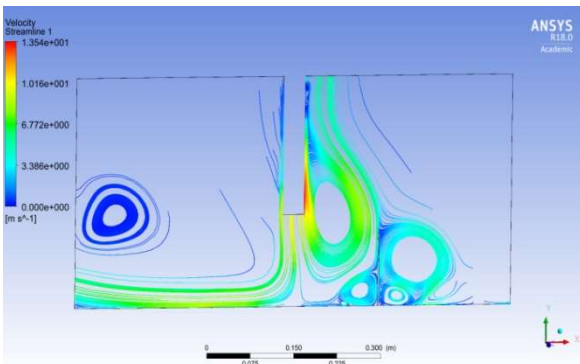
The flow domain dimensions are increased to 10 times than previous case as in original. Dimensions of the transmission pole are kept constant. The transmission pole height of 8 meters which is negligible in comparison to downburst fall height from ground and domain size. So, the comparative height of transmission pole is very less or negligible than of fall height of downburst. The pressure generated by this is coupled in static structural as a multiphysics problem to find different stresses and deflection values.

Figure 10 shows the output of the Fluid Structure Interaction for the pole subjected to impinging jet velocity of 100m/s. The pressure on transmission pole increases drastically, and the deflection generated on transmission pole is as high as 10-11cms, which is large value as it can cause the failure of whole transmission line or the failure of pole from base which further leads to failure of whole transmission line. Moreover, several vortex formation is seen for the steady state solution.

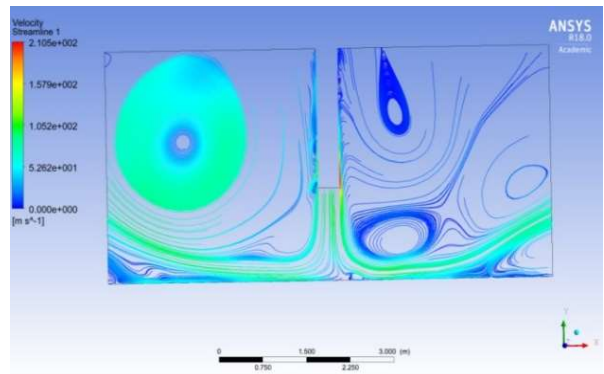


d) Total Deformation

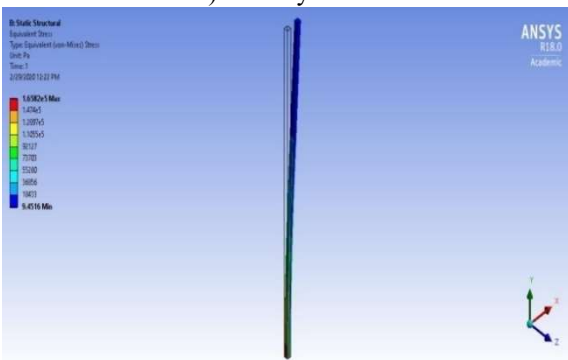
Figure 9. Stress and deflection on transmission pole with downburst jet velocity of 10m/s.



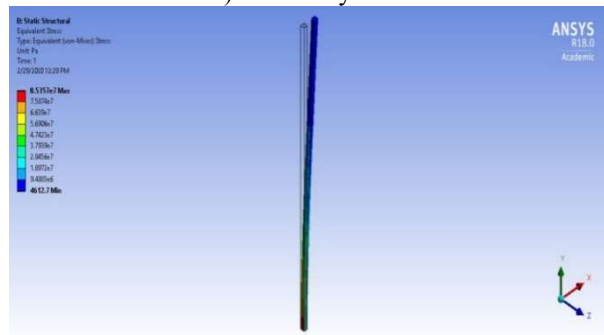
a) velocity streamline



a) Velocity Streamline



b) Von-Mises Stress



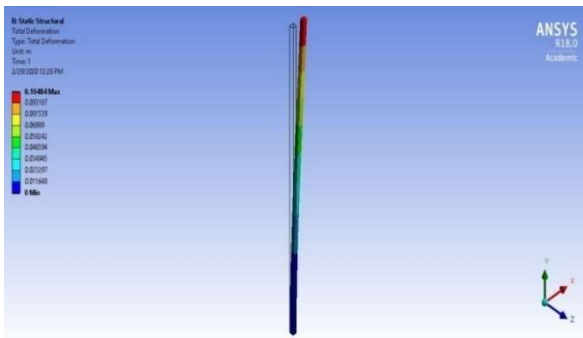
b) Von-Mises Stress



c) Maximum Principal Stress



c) Maximum Principal Stress



d) Total Deformation

Figure 10. Stress and deflection on transmission pole with downburst jet velocity of 100m/s.

4. Conclusions

The one-way coupling fluid structure interaction method is utilised in order to evaluate the stresses and pole deformation that occur during a downburst. The downbursts have been modelled using the impinging jet velocities so that the pressure contour and velocity streamlines can be determined. During a downburst, the impacts of a variety of different viscous models are also investigated for a pole. The evaluation of the fluid domain is done in two dimensions, while the evaluation of the solid domain is done as a three-dimensional Problem. The following inferences can be made based on the findings of the study:

1. The low-pressure vortex begins to form at a location not too far from the opposite extreme of the domain and then moves toward the centre. At the conclusion of the transient analysis, two vortices were identified.
2. Maximum positive pressure is exhibited in the region close to the wall in the steady state solution, whereas maximum negative pressure is shown in the region close to the downbursts.
3. Three viscous models $k - \epsilon$, $k - \Omega$, and the RANS model are used to simulate the effects of a downburst on a transmission pole. The RANS model has been demonstrated to offer more accurate findings than the other two models. Other models also produce results that are somewhat close; additional research can be conducted on any of these models.
4. Because the maximum pressure is observed in the vicinity of the poles in all of the models, the structural design of the poles and towers will be impacted as a result.
5. When the velocity is low, the stresses and deformation of the poles are both relatively modest; nevertheless, when the velocity is increased, both of these physical parameters have a tendency to grow.
6. In the design process, the downbursts loads on large towers needs to be considered to be the predominant load of all the different load combinations. Moreover, it is essential to take into account the structural dynamic properties under downbursts in order to prevent the failure of the structure.

Disclosures

Free Access to this article is sponsored by SARL ALPHA CRISTO INDUSTRIAL.

References

1. Aboshosha, H., & El Damatty, A. (2013). Downburst induced forces on the conductors of electric transmission lines and the corresponding vulnerability of towers failure. *GEN*, 164, 1.
2. Goff, R. C., & Goff, R. C. (1976). Vertical Structure of Thunderstorm Outflows. *Monthly Weather Review*, 104(11), 1429–1440. [https://doi.org/10.1175/1520-0493\(1976\)104<1429:vsoto>2.0.co;2](https://doi.org/10.1175/1520-0493(1976)104<1429:vsoto>2.0.co;2)
3. Gomes, L., & Vickery, B. J. (1978). Extreme wind speeds in mixed wind climates. *Journal of Wind Engineering and Industrial Aerodynamics*, 2(4), 331–344. [https://doi.org/10.1016/0167-6105\(78\)90018-1](https://doi.org/10.1016/0167-6105(78)90018-1)
4. Kim, J., & Hangan, H. (2007). Numerical simulations of impinging jets with application to downbursts. *Journal of Wind Engineering and Industrial Aerodynamics*, 95(4), 279–298. <https://doi.org/10.1016/j.jweia.2006.07.002>
5. Zhang, S., Solari, G., De Gaetano, P., Burlando, M., & Repetto, M. P. (2017). A refined analysis of thunderstorm outflow characteristics relevant to the wind loading of structures. *Probabilistic Engineering Mechanics*, 54, 9–24. <https://doi.org/10.1016/j.probengmech.2017.06.003>
6. Solari, G., Burlando, M., & Repetto, M. P. (2020). Detection, simulation, modelling and loading of thunderstorm outflows to design wind-safer and cost-efficient structures. *Journal of Wind Engineering and Industrial Aerodynamics*, 200, 104142. <https://doi.org/10.1016/j.jweia.2020.104142>
7. Solari, G. (2020). Thunderstorm Downbursts and Wind Loading of Structures: Progress and Prospect. *Frontiers in Built Environment*, 6. <https://www.frontiersin.org/articles/10.3389/fbuil.2020.00063>
8. Babaei, R., Graat, K., Chan, C., & Savory, E. (2021). Experimental simulation of stationary and traveling density-driven thunderstorm downbursts using the two-fluid model. *Journal of Wind Engineering and Industrial Aerodynamics*, 211, 104553. <https://doi.org/10.1016/j.jweia.2021.104553>
9. Canepa, F., Massimiliano Burlando, Djordje Romanic, Giovanni Solari, & Horia Hangan. (2022). Experimental investigation of the near-surface flow dynamics in downburst-like impinging jets. *Environmental Fluid Mechanics*. <https://doi.org/10.1007/s10652-022-09870-5>
10. Shehata, A. Y., El Damatty, A. A., & Savory, E. (2005). Finite element modeling of transmission line under downburst wind loading. *Finite Elements in Analysis and Design*, 42(1), 71–89.
11. Shehata, A. Y., & El Damatty, A. A. (2007). Behaviour of guyed transmission line structures under downburst wind loading. *Wind and Structures*, 10(3), 249–268.
12. Hamada, A., & El Damatty, A. A. (2011). Behaviour of guyed transmission line structures under tornado wind loading. *Computers & Structures*, 89(11–12), 986–1003.
13. Elawady, A., & El Damatty, A. (2016). Longitudinal force on transmission towers due to non-symmetric downburst conductor loads. *Engineering Structures*, 127, 206–226.
14. Ibrahim, A. (2017). Behaviour of Pre-stressed Concrete Transmission Poles under High Intensity Wind. *Electronic Thesis and Dissertation Repository*. <https://ir.lib.uwo.ca/etd/5029>
15. Ahmed, M., Damatty, A. A. E., Dai, K., Ibrahim, A., Ibrahim, A., & Lu, W. (2022). Parametric study of the quasi-static response of wind turbines in downburst conditions using a numerical model. *Engineering Structures*, 250, 113440. <https://doi.org/10.1016/j.engstruct.2021.113440>
16. FLUENT 6.0 User's Guide. 2001. vol. 1–4. Fluent Inc., Lebanon, December 2001.
17. Launder, B. E. (1989). Second-moment closure and its use in modelling turbulent industrial flows. *International Journal for Numerical Methods in Fluids*, 9(8), 963–985.